Looking by grazing incidence small angle x-ray scattering at gold nanoparticles supported on rutile TiO_2(110) during CO oxidation

M.-C. Saint-Lager[1], A Bailly[1], M. Mantilla[2], S. Garaudée[1], R. Lazzari[2], P. Dolle[1], O. Robach[3], J. Jupille[2], I. Laoufi[1], P. Taunier[1]

[1] Institut Néel, CNRS & Université Joseph Fourier, 25 Avenue des Martyrs, F-38042 Grenoble Cedex 9, France
[2] Institut des NanoSciences de Paris, Université Pierre et Marie Curie Paris 6, UMR 7588 CNRS, Campus Boucicaut, 140 Rue de Lourmel, F-75015 Paris, France
[3] Nanostructures et Rayonnement Synchrotron, Commissariat à l'Energie Atomique, 17 Avenue des Martyrs, F-38054 Grenoble, Cedex 9, France

Abstract

The catalytic activity of oxide-supported gold nanoparticles depends crucially on their size. The present work describes a dedicated set-up in which particle size is determined by grazing incidence small angle x-ray scattering (GISAXS) and reactivity is analysed via a mass spectrometer. Catalytically active gold nanoparticles supported on TiO_2(110) of size ranging between 2.4 and 5 nm were characterized during the CO oxidation at pressures in the range 0.1-100 mbar. The growth was found 3D and the particles were best modelled by a truncated sphere. The reaction rate per Au atom measured at 470 K was seen to increase in a monotone manner as the cluster size decreases, without reaching any maximum. Particles of size lower than 3 nm were stable under oxygen but sintering occurs when CO is added at 470K. That dimension coincides with the switch which was previously observed from nucleation-growth, with particles pinned on defects, to coalescence where particles become independent of defects.

Introduction

Supported gold nanoparticles exhibit unexpected reactive properties with respect to bulk gold. Considered as the noblest metal, bulk gold does not react with simple molecules such as oxygen because of the repulsion between the filled *d* orbital of the metal and the molecular orbital of the adsorbates. Therefore, it is a very poor catalyst for hydrogenation and oxidation [1]. The striking behaviour is that nanometer-size gold particles supported on oxide show a surprisingly high catalytic activity [2][3] even at room temperature and below. Such property might, for instance, be used for the low-temperature selective oxidation of carbon monoxide (CO) which is required to remove CO traces in the hydrogen flow in fuel cells so as to prevent the poisoning of the Pt catalyst [4].

Concerning the sites for CO adsorption on the Au/TiO_2 catalyst, it is generally accepted that CO sits on the gold particles themselves. Edges or step sites are often invoked [5]. However, adsorption on gold facets was also suggested by Reflection Absorption InfraRed Spectroscopy (RAIRS) experiments on an Au(111) single crystal since, at RT and above 1 Torr, CO molecules are linearly chemisorbed on top of gold atoms [6]. The main open question is how oxygen adsorbs and dissociates since it usually does not interact with bulk gold. Meyer et al. have summarized as follows the different ideas proposed to explain the exceptional activity of gold nanoparticles for CO oxidation [7]:

(i) the presence of highly uncoordinated gold atoms promotes the oxygen adsorption and/or dissociation;
(ii) the chemical properties of the nanoparticles are the consequence of the quantum size effect with the opening of a bandgap. The corollary is that the thickness of the gold particle is the critical parameter;
(iii) the active site for gold catalysis involves Au^+ cation whose presence may result from the catalyst precursor or the calcination treatment;
(iv) the active site for gold catalysis is an anionic gold (Au^-) species which results from the interaction of a particle with a F centre defect (due to an oxygen vacancy) in the underlying oxide support and which allows the adsorption (and possible dissociation) of oxygen;
(v) the active site for catalysis involves the interface between the particle and support. For CO oxidation it is generally proposed that CO adsorbs on the surface of the gold particle whereas oxygen adsorbs on the metal oxide support and moves to the particle/support interface or adsorbs there directly.

The two first explanations are "gold-only" route for CO oxidation. They mainly stem from experiments performed on

model catalysts elaborated in ultra high vacuum (UHV) and which can be considered as surface science type [8]. They both suppose a link between the reactivity and the particles size. Indeed, a general finding is that the reactivity of gold particles increases dramatically as their size decreases [9]. For most of the authors this increase is continuous [5]. Lopez and co-workers compared experimental data of several groups over gold supported on different reductible and nonreductible oxides. They concluded that the most important effect comes from the availability of many low coordinated gold atoms (explanation (i)) [10]. However, a maximum in turnover frequency (TOF) was observed for gold clusters of 2.5 to 3 nm- diameter deposited at the surface of a rutile crystal [11]. It was attributed to a quantum size effect (explanation (ii)) with the activity maximum occurring for two-atoms-thick clusters [11]. The size dependence of the activity was later studied by other techniques such as Extended X-ray Absorption Fine Structure (EXAFS) [12]. No evidence was found for maximum activity for small particles, but the determination of the particles size becomes more uncertain when particles are smaller than 3 nm. On high-area catalysts, the gold particles are most often produced by wet chemistry. Ionic gold atoms, such as in (iii) and (iv), are a common finding in much of the published research in this field.

The size of the particles and the charge transfer between the oxide and the particles appear as the dominant factors of the catalytic activity of supported gold particles [13]. Both are suggested to depend on the preparation method. Even the sign of the charge transfer can change when switching from Ti-rich to Oxygen-rich titanium oxide surface [13]. However, for all catalysts, the catalytic activity of supported gold particles is associated with sizes in the nanometer range.

A constant need in understanding the catalytic behaviour is thus the determination of the size, structure and chemical state of the clusters *in operando* or, at least, *in situ*, so as to bridge the so called "pressure gap" between ultra-high vacuum and normal conditions. To get informations about the shape, the size and the density of supported nanoparticles, a relevant technique is Grazing Incidence Small Angle X-ray Scattering (GISAXS). The present paper is devoted to the *in operando* study of TiO_2-supported gold nanoparticles by GISAXS to establish a link between the morphology of the particles and their catalytic activity during the reaction of oxidation of the carbon monoxyde.

Experimental setup

The principle of the GISAXS is depicted in figure 1. A narrow and well-collimated incident X-ray beam is impinging on the surface at a grazing angle, close to the critical angle for total external reflection. The scattered intensity is recorded around the origin of the reciprocal space. Because of small scattering angles, the measurement is sensitive only to the mean electronic density and not to the atomic arrangement. The signal is collected on a 2D detector close to the direct beam. The GISAXS pattern of a disordered collection of particles exhibits two halos on each side of the specular rod. To first order, the GISAXS intensity is proportional to the form factor $F(\mathbf{Q})$ times the interference function $S(\mathbf{Q})$, where $\mathbf{Q}$ is the momentum transfer. $F(\mathbf{Q})$ and $S(\mathbf{Q})$ are respectively the Fourier transforms of the particle shape and the island-island pair correlation function. The average island separation D is inversely proportional to the distance between

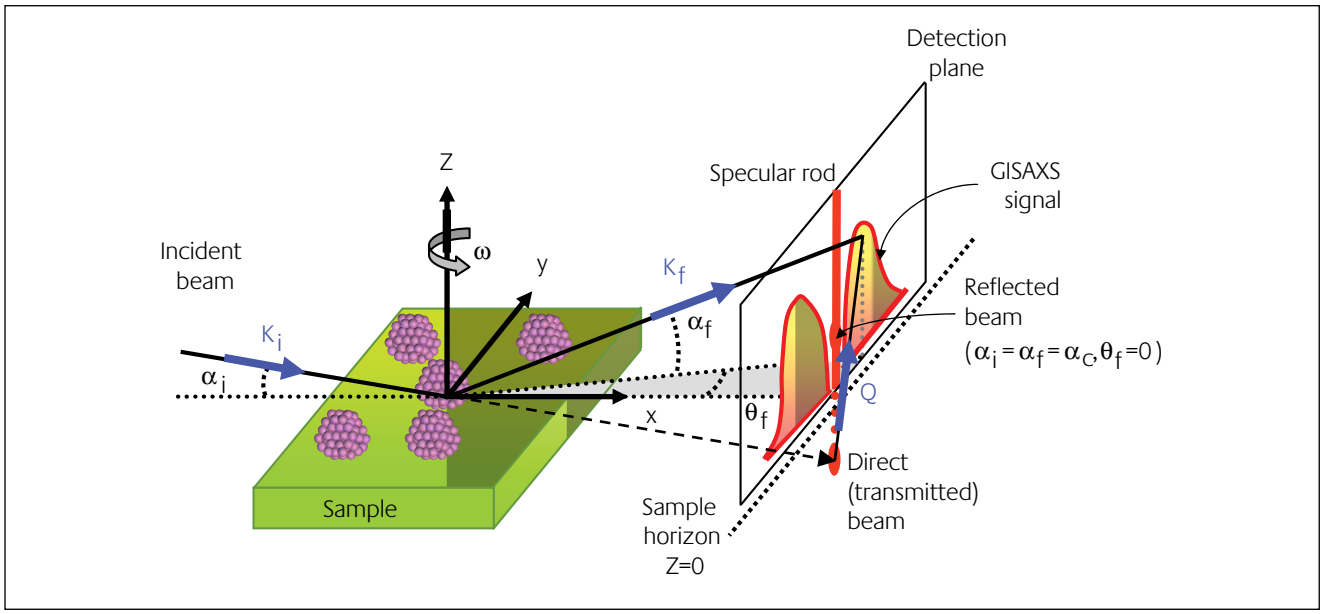

Figure 1

Experimental scattering geometry for GISAXS. $\mathbf{K}_i$ is the wave vector of the incident photons and α_i the angle with respect to the surface sample; the wave vector of the scattering beam is $\mathbf{K}_f$, with θ_f and α_f as in- and out of plane angles. $\mathbf{Q}$ is the momentum transfer. ω is the sample rotation around its surface normal, which defines the X-ray beam orientation with respect to the in-plane crystallographic directions. The bidimensional detector is in a plane perpendicular to the surface. The GISAXS signal is on each side of the central direct and reflected beams

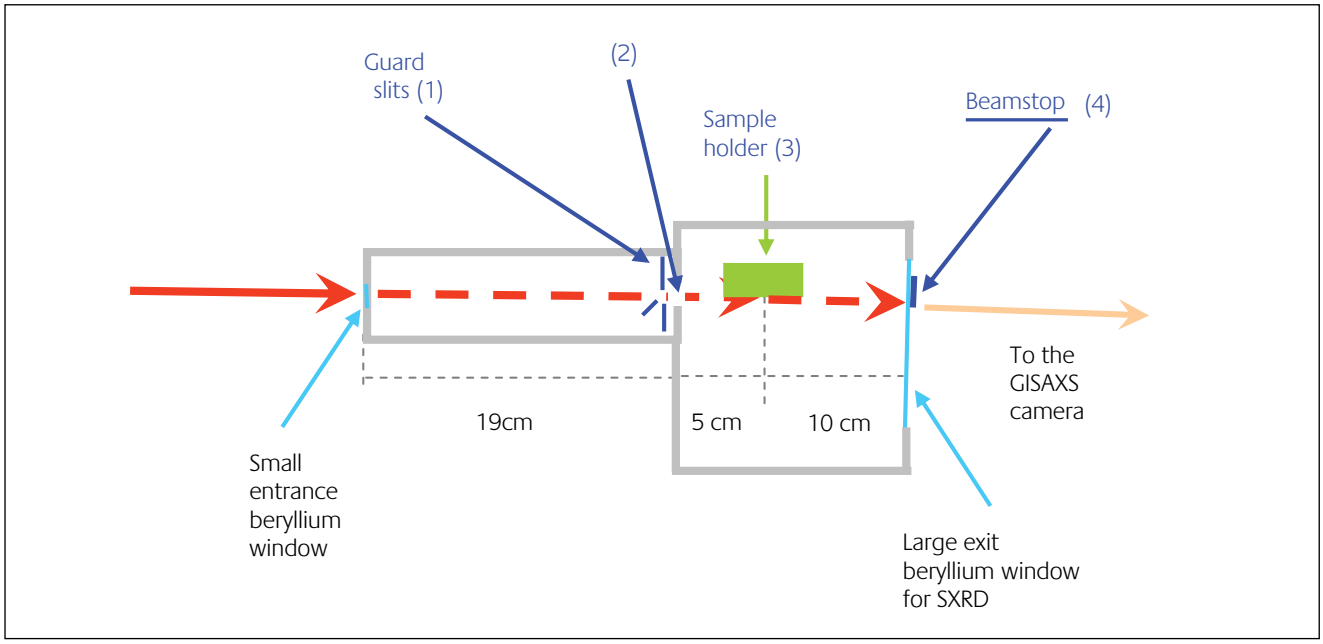

Figure 2

Schematic representation of the beam-path for GISAXS in the YZ plane perpendicular to the sample surface. First the beam crosses the small entrance Beryllium window to come into the reactor, then it goes through the guard slits (1) and through the opening (2) before colliding the sample surface (3). The diffracted beam goes out the reactor through the large exit beryllium (needed for GIXS), and the beam-stop (4) is mounted behind this window and very close to it. All the distances are optimized to take into account the geometric constraints of the set-up and to minimize the scattering by the beryllium windows and by the reactive gas in the reactor

the halos along the Q_y parallel direction [14]. The particle lateral average size *d* and height *h* are thus inversely proportional to the spread of the scattering, parallel and perpendicular to the surface, respectively [15]. Scattering angles in the range of a few degrees correspond to wave vector transfers **Q** that probe nanometric distances. Sensitivity to particle shape is achieved by analyzing the power law decrease of the intensity far away in reciprocal space, in the Porod regime [16]. With incident and exit angles close to the critical angle, the modelling of the GISAXS intensity within the kinematical approximation, or Born approximation, is inadequate. The model has to be modified to account for reflection and refraction effects, leading to the so-called distorted-wave Born approximation [17, 18]. The formalism was included in the *IsGISAXS* program [19]. Interference functions between particles are taken into account either in the decoupling approximation, where sizes and positions are not correlated, or in the local monodisperse approximation. Several simple island shapes have also been implemented.

A new experimental set-up combining grazing incidence X-ray diffraction (GIXRD), GISAXS and reactivity measurements was built to study complex surfaces such as thin epitaxial films or supported nanoparticles. It has been described in details elsewhere [20]. It is made of two connected UHV chambers. The sample can be transferred from the one to the other by a mechanical transfer rod, in UHV environment. The model catalysts can be prepared just before the X-ray experiment, in the UHV chamber equipped for surface preparation and with the usual probes for surface analysis (Auger spectroscopy and Low Energy Electron Diffraction). The second chamber is dedicated to both X-ray and reactivity measurements [20]. Since the GISAXS signal is lower than the incident beam intensity by more that ten orders of magnitude, the diffuse background must be decreased as much as possible. In this respect, two elements are crucial: the guard slits before the sample and the beam stop after it to avoid the direct beam to saturate the camera. A sketch of the beam path is represented in figure 2. This geometry allows GISAXS analysis with a good signal to noise ratio for gold coverage as low as 0.4 monolayer (ML).

The x-ray scattering experiments have been performed on the GMT station at the BM32 bending magnet beamline of the European Synchrotron Radiation Facility (ESRF in Grenoble, France). The *in situ* apparatus is set on the "2+2" diffractometer of the GMT station. It is equipped with a goniometer head allowing a precise positioning of sample surface for grazing geometry. The X-ray energy was equal to 18 keV, which corresponds to a wavelength λ=0.6888Å. At this energy, the absorption and fluorescence from the TiO_2 substrate and the gold film are negligible. The incidence angle was fixed at α_c=0.13° (critical angle of TiO_2 for total external reflection at the corresponding energy). A shutter was mounted to avoid damaging the surface by an over-exposition to the X-ray beam. It was only opened during X-ray data collection. Finally, no significant difference could be observed in either the scattering or the catalytic activity with and without photons on the sample. The GISAXS signal was collected on a Peltier cooled 16-bit 1-Mpixel charge-coupled device camera (Princeton, Instruments, pixel size of 56.25 µm). It is located 1.25 meter away from the surface sample, except for the 0.7nm thick gold film for which it was put further away at 1.65 m. Images were corrected from *(i)* dark counts, *(ii)* flat

field, *(iii)* camera distortion. Since GISAXS patterns are nearly independent from azimuthal rotation, the analysis was restricted to data collected with the X-ray beam aligned along the $[1\text{-}10]_{TiO2}$ direction.

The TiO_2(110) cylindrical crystal (diameter 14 mm, thickness 1.5 mm), used as substrate, was supplied chemo-mechanically polished with the lowest possible roughness (R_a=0.5 nm) and a miscut lower than 0.1°. It was fixed on the sample holder by tungsten clips. Its surface was cleaned by bombardment with a 800 eV Ar+ ion beam. It was then annealed ten minutes at 1000 K under 10^{-5} mbar O_2, followed by a cooling in oxygen, following protocols that were shown to minimize the defect concentration of the rutile surface [21]. The Au film was grown in the UHV preparation chamber. High purity gold was evaporated on the surface from a cell held at 1470 K. The evaporation rate (0.1 nm/min) was calibrated by a quartz microbalance. The temperature was estimated by an IR pyrometer [20]. Gold thickness equivalent to 0.1 ML up to 3 ML were explored; 1ML corresponding to a single Au(111) closed-packed atomic layer (0.235 nm- thickness). Gold deposition was performed according to a previous GISAXS study establishing the relationship between the size of gold nanoparticles grown on TiO_2(110) and the coverage *t* [22]. Following this work, the range of coverage explored herein (0.1 to 3 ML) corresponds to clusters of diameter *d* ranging between 1,5 and 6 nm. This range is expected to be the most relevant with respect to the activity of Au nanoparticles for CO oxidation [11]. After gold deposition, the sample was transferred in the reactor in vacuum environment. GISAXS was performed under several conditions: under oxygen or CO pressures between 1 to 100 mbar, as well as under CO + O_2 reactive mixture (total pressure 10 to 20 mbar). In all cases, the photons scattered by the gas phase was negligible except for a pressure equal to 100 mbar for which the noise level on GISAXS patterns increased significantly.

The reactivity was monitored by analyzing the gas phase by means of a mass spectrometer connected to the reactor through a leak valve. The requirements due to the coupling of GISAXS and GIXRD yield to a static reactor with a relatively large volume (ca 6 litres). Gas, with the best available purity, were used: N55 for oxygen and N37 for CO. The environment of the sample in the reactor was designed to be chemically passive. The whole gas manifold is made of stainless steel. It was backed out and pumped down to 10^{-7} mbar. Special care was taken in order to avoid nickel deposition on the surface through decomposition of nickel carbonyls known as possible contaminants of CO. Indeed, this has a dramatic effect, especially on gold surfaces. $Ni(CO)_4$ dissociates at around 500K. CO was thus purified by heating; we observed that, to remove the pollutant of CO that forbids the CO oxidation, it was necessary to raise the temperature up to 550K during a few minutes.

For gold supported on an oxide single crystal, the amount of active atoms is small. Typically, for a substrate surface of 1 cm^2, a gold coverage equivalent to 1ML involves $1.4.10^{15}$ atoms corresponding to a weight of 0.5 µg, if assuming an atomic arrangement similar to an Au(111) plane. The rate of CO conversion on gold nanoparticles is frequently observed around a few mmoles per gram per second. When 0.1 mbar is introduced in the reactor, 25% of the CO is expected to be converted in one hour if the rate is 4 mmole/g/s. This is typically what it is possible to measure in our setup.

In operando study of gold nanoparticles on TiO_2 (110)

During the experiment, clusters of different sizes were exposed to various conditions, including ultra-high vacuum, oxygen environment and, finally, oxygen and CO mixture. Data were mostly collected after transfer in the X-ray reactor chamber, during a procedure which involved the following steps: (1) the as deposited gold clusters, in UHV and at room temperature (RT); (2) during exposure to 20 mbar of oxygen; (3) after adding 0.1 mbar of CO; (4) after pumping down to UHV; (5) after increasing the temperature at 470 K, in UHV; (6) during exposure to 20 mbar of oxygen at 470 K; (7) after adding 0.1 mbar of CO – also at 470 K; (8) after pumping down to UHV. Each step was about two hours long. The reactivity was analyzed by recording the signals of oxygen (mass 32 and 16), CO (mass 28) and CO_2 (mass 44 and 28) with the mass spectrometer [20]. We also monitored the mass 18, associated with water vapour, since water can influence the growth of gold on TiO_2(110) and its reactivity.

Cluster sintering: GISAXS results

Figure 3 shows the evolution of GISAXS patterns as a function of the equivalent gold thickness at room temperature. The two lobes of diffuse scattering located on each side of the beam stop are the so-called correlation peaks. Upon increasing the average film thickness, they progressively shrink towards the origin of the reciprocal space. This is indicative of an increase in diameter d, height h and separation distance D of the gold clusters. The data fits give the parameters shown in Table 1. The methodology of modelling is similar to that followed in Ref. 22; in particular, the analysis was performed by modelling the gold clusters by a truncated sphere. Notably, the aspect ratio (h/d) remains about constant and its values (0.55 to 0.65) are close to those previously observed in this range of thickness (0.4 to 3 ML) for Au/TiO_2(110) [22].

The GISAXS patterns were then recorded during the above mentioned gas exposures, as illustrated in figure 4 in the case of the 0.1 nm (0.4 ML) equivalent thickness. These images evidence that particles do not undergo any change upon exposures at room temperature. To confirm this result, a larger range of pressure to suppress was explored. No change was observed by GISAXS under CO or O_2, whatever the partial pressure between 1 and 100 mbar was. Exposures to the CO + O_2 mixture (total pressure 10 to 20 mbar and CO:O_2 pressure

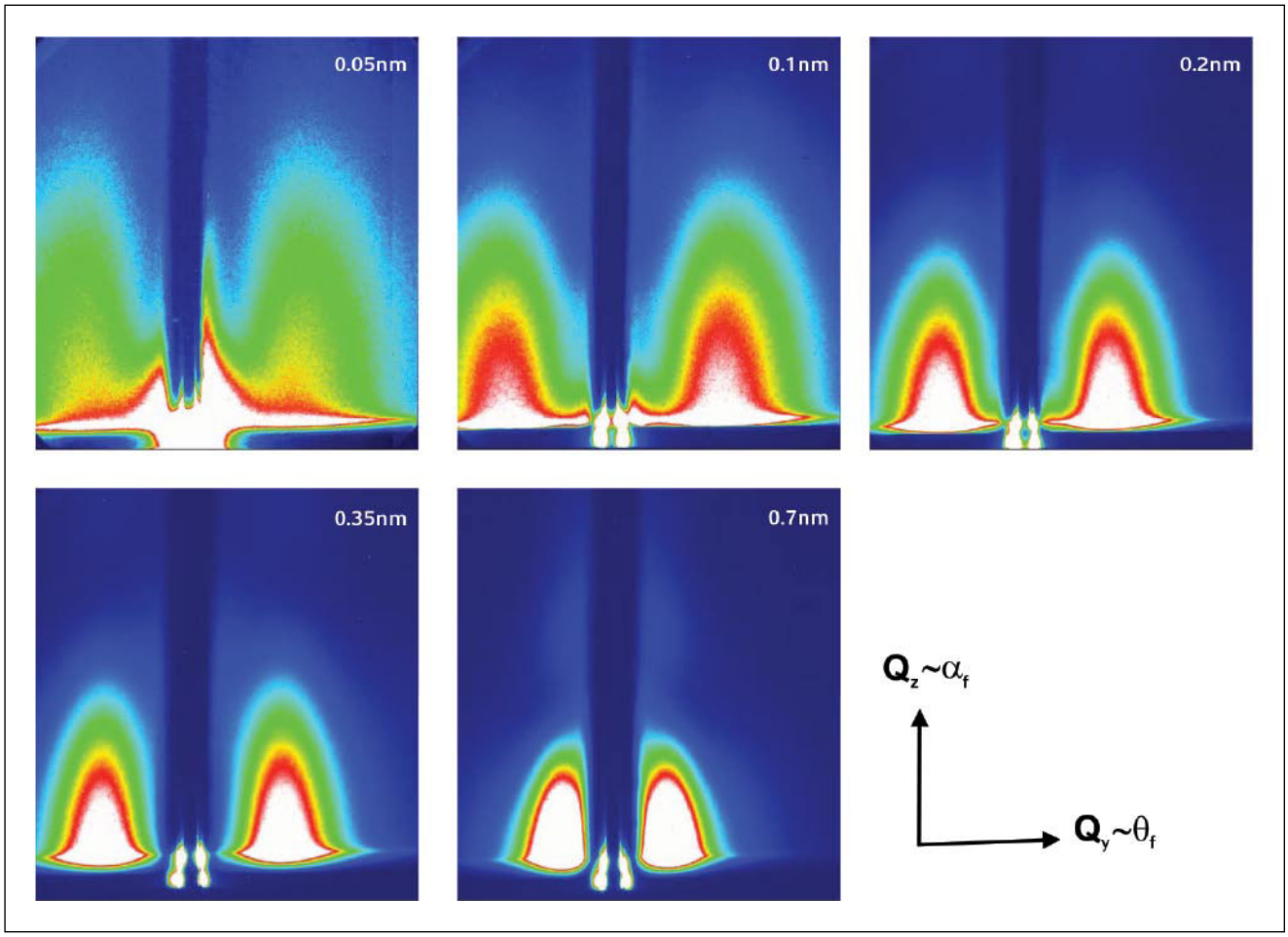

Figure 3

GISAXS patterns for several Au equivalent thicknesses measured in UHV at room temperature (from 0.05 nm (0.2ML) up to 0.7 nm (3ML) measured in UHV at room temperature

ratios between 1:2 and 1:100) had no effect either. Moreover, under these conditions, no reaction could be detected.

At 470 K, the particles remained stable in UHV and under 20 mbar oxygen but the system strongly evolved when a partial pressure of CO (0.1 mbar) was added to the oxygen at 20 mbar. In parallel, the CO oxidation was detected. This will be described in the next part. The parameters characteristic of the morphology of the film which were recorded after 2 hours under 20 mbar O_2 + 0.1 mbar CO are given in Table 1. The cluster size d increases while their density ($\sim D^{-2}$) decreases and their aspect ratio h/d remains stable. For gold coverage higher than 1ML no change was observed even at 470K. This thickness corresponds to clusters with diameter larger than 3 nm. However, as we will see, some CO conversion into CO_2 was observed in these conditions.

Catalytic activity towards CO oxidation

In a similar manner as in the work of Schumacher *et al* [23], a large ratio P_{CO}/P_{O2} (200) must be used to measure the catalytic activity in good conditions. The CO conversion into CO_2 was analysed at 470K under partial pressures P_{O2} = 20 mbar and P_{CO} = 0.1 mbar. However, most reactivity measurements performed *in situ* at synchrotron were not performed over long enough periods to derive accurate data. Therefore, experiments were performed again in the laboratory with the same setup. The conditions of the measurements were carefully reproduced regarding the preparation of the sample, the gold evaporation, as well as the sequence of treatments for which similar temperatures, partial pressures and durations were used.

Figure 5a shows the CO transformation into CO_2 as a function of time for several gold equivalent thicknesses (from 0.1 ML to 3ML) at 470K. These data are derived from the analysis of the mass 28 and 44 recorded by the mass spectrometer. A curve measured during experiment at ESRF is also reported on the same plot, which confirms that the experimental conditions of measurements at synchrotron were well reproduced at the laboratory. The data were first corrected from the signal recorded before the introduction of the gas in the chamber. Then they were calibrated by taking into account the ionization factor and fragmentation of the CO and CO_2 molecules. As a matter of reference, the background was measured without gold on TiO_2. Figure 5b gives the variation of the reaction rate, taken at the beginning of the exposure, as a function of the equivalent gold thickness. It is expressed as (rate of production of CO_2 molecules)/(total Au atoms)/second [11]. Within the coverage

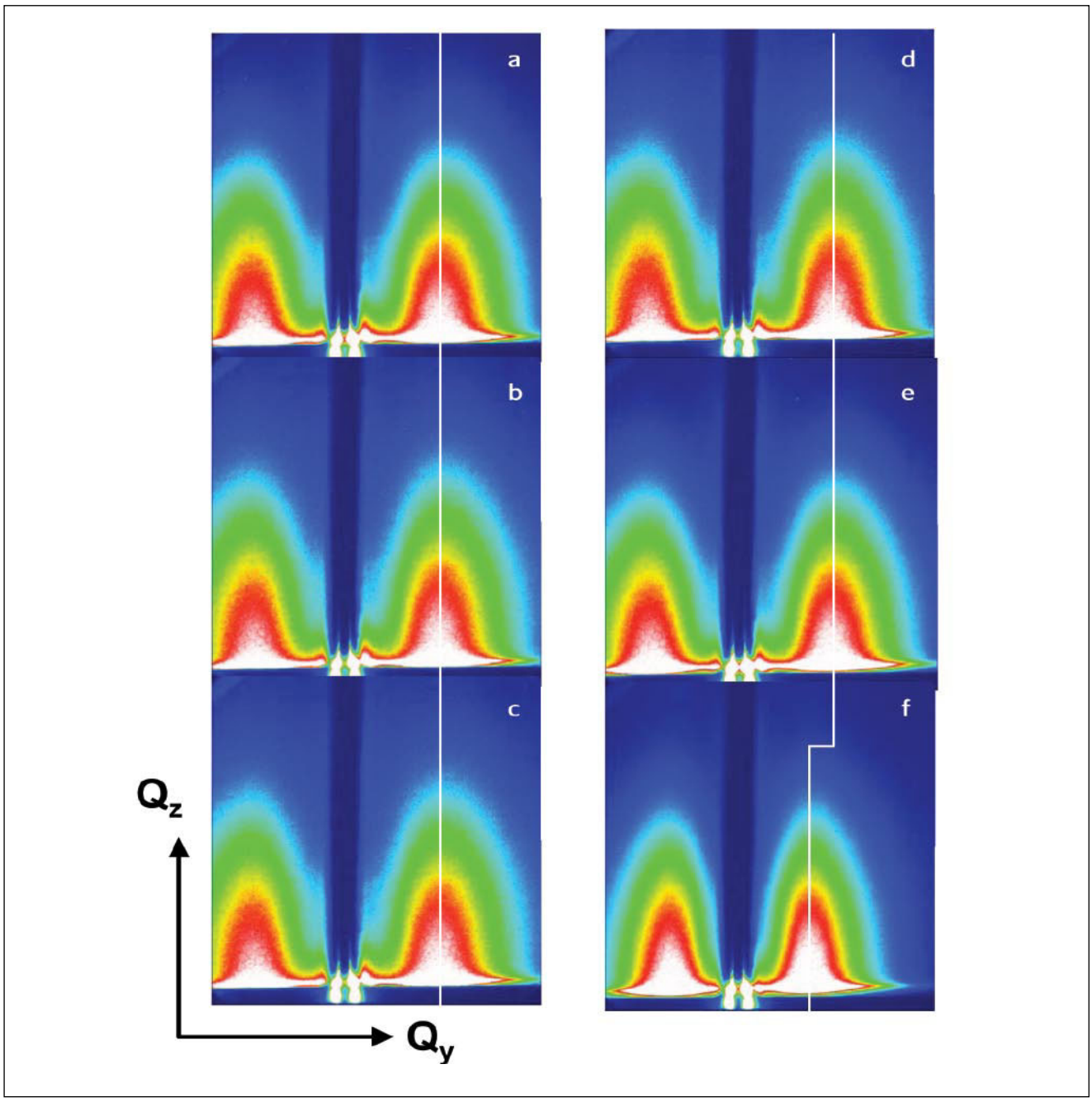

Figure 4:
GISAXS patterns recorded for the 0.1 nm (0.4 ML) equivalent thickness (a) in UHV at room temperature (RT), (b) under 20 mbar O_2 at RT, (c) under 20 mbar O_2 + 0.1 mbar CO at RT; (d) in UHV at 470K, (e) under 20 mbar O_2 at 470K, (f) under 20 mbar O_2 + 0.1 mbar CO at 470K. The vertical white line indicates the evolution of the centre of the lobe.

range used herein, the activity strongly increases when the deposited gold amount decreases from 3 to 0.1 ML. The corresponding size of gold clusters, as deduced from GISAXS analysis, are also reported on figure 5b, showing that measurements extend from diameter smaller than 2.4 nm up to size close to 5 nm.

Discussion

The present work opens the possibility of the determination of a direct relationship between the size and the reactivity of the gold particles. GISAXS measurements were previously proved to provide accurate values of the parameters which characterize the size and the shape of supported particles, thus leading to a definition of what can be called an 'average' particle in the case of a vast collection of nanoparticles [18,22].

The temperature used to test the catalytic oxidation of CO on the Au/TiO_2(110) film was set at 470 K. It was chosen to achieve high enough reaction rates to allow measurements in good conditions. That rather high temperature is a likely explanation of values of the turnover frequency found higher than those observed by either Schumacher *et al.* [23] or Valden *et al.* [11] who have performed measurements at 350 K. The range of particles diameter which has been explored herein spans from 2.4 nm to 5.2 nm. A very important

Table1

Morphological parameters obtained from GISAXS patterns analysis : diameter (d), distance between particles (D) and aspect ratio height/diameter h/d

Gold equivalent thickness (nm) ±0.02 nm	Conditions	d (nm) ±0.7	D (nm) ±0.5	h/d ±0.1
0.7 (3ML)	UHV - RT	5.2	7.7	
0.35 (1.5ML)	UHV – RT	3.2	5.5	0.6
	reaction – 470K	3.2	5.5	0.6
0.2 (0.8ML)	UHV-RT	2.9	5.3	0.65
	reaction – 470K	3.8	6.5	0.55
0.1 (0.4ML)	UHV – RT	2.4	4.0	0.6
	reaction – 470 K	2.8	5.1	0.6

observation is that, within the whole range of our measurements, the reactivity clearly increases in a monotone manner as the size of the particles decreases, without any apparent maximum. Such an observation differs from that of Valden *et al*. who have concluded from a Scanning Tunnelling Microscopy (STM) study that, for the same system, the turnover frequency passes through a maximum for a particle size of 3 nm [11]. In addition, as estimated by GISAXS, the the particles studied herein were found thicker than the two-layers thick clusters which were described as the more reactive gold particles [11]. Attempts to model the gold particles by two-layers high flat-top clusters lead to very bad fits with respect to either cylindrical shape or truncated spherical shape. The latter models, both fitted with free heights, lead to similar values of the morphological parameters, though the truncated sphere model was finally chosen because it allowed slightly better fits. Clearly, in the present case, the cluster size at which the metal to nonmetal transition occurs [13] is lower than 2.4 nm.

A sintering of gold particles smaller than 3 nm was observed at 470 K under the CO + O_2 reactive mixture, as the catalytic activity increases strongly with decreasing particle size. However, annealing the same clusters in vacuum or in oxygen atmosphere at the same pressure had no effect on the particle size. A similar behavior was observed for gold over cerium oxide [24]. Sintering under the reactive mixture has been already reported for Au/TiO_2 [25]. An oxygen-induced sintering was observed [26] in the same conditions

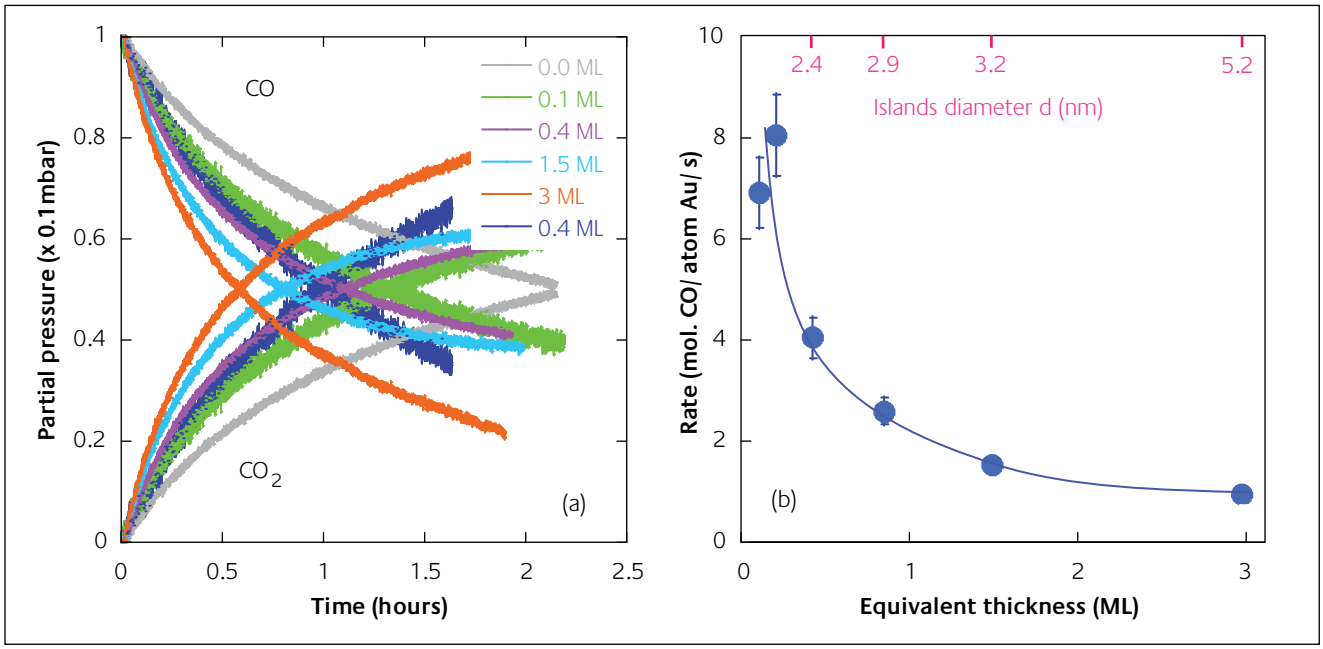

Figure 5

Activity of the gold islands as a function of the Au film thicknesses for the mixture 10 mbar O_2 + 0.1 mbar CO.

(a) CO and CO_2 partial pressures as a function of time for several thicknesses, CO and CO_2 pressures starting from one and zero, respectively. They were deduced from the mass 28 and 44 measured by the mass spectrometer. The dark blue curves correspond to data collected for 0,4 ML during the x-ray experience, the grey ones to those obtained without gold on the TiO_2(110) support.

(b) Atomic rate of CO conversion into CO_2 as a function of the film thickness of the deposit. The background measured on the bare substrate has been subtracted. The measured diameters are reported on the top horizontal axis. The solid line is a guide for eyes.

of pressure and temperature than in the present work, though with a different substrate preparation, since annealing after argon sputtering was performed in UHV instead under oxygen. Notably, the size of 3 nm of the gold particles corresponds to the switch from growth to coalescence which is observed during the deposition of the Au/TiO_2(110) film [22]. Below that limit, the particle distribution is consistent with a pinning by surface defects of about a constant number of growing particles. At higher coverage, the film obeys a dynamic model in which the inter-particle distance is proportional to the particle size and is no longer connected to defects. The number of particles is rapidly decreasing at that stage. The adsorbate-induced sintering might be less effective in the region (> 3nm) where supported clusters have already undergone a coalescence. Finally, the high reactivity observed for particle size lower than 3 nm can be associated with particles pinned by defects. That behavior supports the idea that defects play a strong role in the catalytic properties [5, 27].

Conclusion

In catalysis by gold nanoparticles, the activity of the supported gold critically depends on the cluster size. The present work illustrates the capability of a dedicated set up to directly determine the particle size by X-ray diffraction at small angles (GISAXS) and to simultaneously characterize the reactivity at pressures up to normal via a controlled leak towards a mass spectrometer.

Au/TiO_2 (110) particles of 2.4 to 5 nm in diameter, deposited in vacuum conditions, were characterized during the reaction of oxidation of CO at partial pressures ranging between 0.1 and 100 mbar with the following main conclusions:

- the reaction rate per Au atom measured at 470 K increases in a monotone manner as the cluster size decreases, without reaching any maximum;
- at 470 K, sintering of particles of size lower than 3 nm was observed in the presence of the CO + O_2 mixture. That size coincides with a previously observed switch from growth with particles pinned on defects to coalescence where particles are independent of defects. At the same temperature, the sintering did not occur under oxygen.

Acknowledgements

The technical staff (SERAS and MCMF) of Institut Néel-CNRS is gratefully acknowledged for their help as well as the staff of the BM32 CRG beam-line. The authors also acknowledge J.P. Simon (Science et Ingénierie des Matériaux et Procédés Grenoble) for fruitful discussions. They also thank ESRF and their committees for beam time allocation.

References

1 B. Hammer and J.K. Norskøv, *Nature*, 1995, **376**,238
2 M. Haruta, *Catal. Today* 1997, **36**, 153
3 M. Haruta, T. Kobayashi, H. Sano and N. Yamada, *Chem. Lett.* 1987, **2** 405
4 S. Arrii, F. Morfin, A.J. Renouprez and J.L. Rousset, *J. Am. Chem. Soc.* 2004, **126**, 1199
5 M. Haruta, *CATTECH*, 2002, **6**, 102
6 L. Piccolo, D. Loffreda, F.-J. Cadete Santos Aires, C. Deranlot, Y. Jugnet, P. Sautet and J.-C. Bertolini, *Surf. Sci.* 2004, **566–568** , 995
7 R. Meyer, C. Lemire, Shaikhudinov and H.-J. Freund, *Gold Bulletin*, 2004, **37**, 72 and references therein
8 J.G. Wang and B. Hammer, *Topics in Catal.*, 2007, **44**, 49
9 F. Bocuzzi, A. Chiorino, S. Tsubota and M. Haruta, *J. Phys. Chem.* 1995, **100**, 3625 and references therein
10 N. Lopez. T.V.W. Janssens, B.S. Clausen, Y. Xu, M. Mivrikakis, T. Bligaard and J.K. Norskøv *J. Catal.* 2004, **225**, 86
11 M. Valden, X. Lai and D.W. Goodman, *Science* 1998, **281**, 1647
12 Overburry, V. Schwartz, D.R. Mullins, W. Yana and S. Dai, *J. Catal.* 2006, **241**, 56
13 K. Okasaki, S. Ichikawa, Y. Maeda, M. Haruta and M. Kohyama, *Applied Catalysis A*: General, 2005, **291**, 45
14 J.R. Levine, J.B. Cohen, Y.W. Chung and P. Georgopoulos, *J. Appl. Cryst.* 1989, **22**, 528
15 J.R. Levine, J.B. Cohen and Y.W Chung, *Surf. Sci.* 1991, **248**, 215
16 In « Théorie et technique de la radiocristallographie, A. Guinier , Eds Dunod Paris 1964
17 M. Rauscher, R. Paniago, T.H. Metzger, Z. Kovatz, J. Domke, J. Peisl, H.-D. Pfannes, J. Schulze and I. Eisele, *J. Appl. Phys.* 1999, **86**, 6763
18 C. Revenant, F. Leroy, R. Lazzari, G. Renaud, and C.R. Henry, *Phys. Rev. B*, 2004, **69**, 035411
19 R. Lazzari, *J. Appl. Crystallogr.* 2002, **35**, 406. ISGISAXS can be downloaded with a user guide from http://www.insp.upmc.fr/axe2/Oxydes/IsGISAXS/isgisaxs.htm
20 M.-C. Saint-Lager, A. Bailly, P. Dolle, R. Baudoing-Savois, P. Taunier, S. Garaudée, S. Cuccaro, S. Douillet, O. Geaymond, G. Perroux, O. Tissot, J.-S. Micha, O. Ulrich, and F. Rieutord , *Rev. Sci. Instrum.* 2007, **78**, 083902
21 V.E. Henrich and A.F. Cox, The surface science of metal oxides, Cambridge University Press, Cambridge, England, 1993; J. Danger, H. Magnan, D. Chandesris, P. Le Fèvre, S. Bourgeois, J. Jupille, R. Gotter, A. Verdini and A. Morgante, *Phys. Rev. B* 2001, **64**, 45110
22 R. Lazzari, G. Renaud, J. Jupille, and F. Leroy, *Phys. Rev. B*, 2007, **76**, 125412
23 B. Schumacher, Y. Denkwitz, V. Plzak, M. Kinne and R.J. Behm, *J. Catal.*, 2004, **224**, 449
24 J.L. Lu, H.-J. Gao, S. Shaikhutdinov and H.-J. Freund, *Catal. Lett.* 2007, **114**, 8
25 X. Lai and D.W. Goodman *J. Mol. Catal A*, 2000, **162**, 33.
26 A. Kolmakov and D.W. Goodman *Catal. Lett.* 2000, **70**, 93; A. Kolmakov and D.W. Goodman *Surf. Sci.* 2001, **490**, L597
27 R.H. Griesel and B.E. Nieuwenhuys, *J. Catal.*, 2001, **199** , 48